

Measurement of the exclusive light hadron decays of the ψ'' in e^+e^- experiments

P. Wang, X.H. Mo, and C.Z. Yuan

Institute of High Energy Physics, Chinese Academy of Sciences, Beijing 100049, China

(Dated: August 23, 2018)

The measurement of the exclusive light hadron decays of the ψ'' in e^+e^- experiments with significant interference between the ψ'' and non-resonance continuum amplitudes is discussed. The radiative correction and the Monte Carlo simulation are studied. A possible scheme to verify the destructive interference is proposed for the detectors with energy-momentum resolution of $(1 \sim 2)\%$.

Keywords: ψ'' exclusive decay; interference; Monte Carlo simulation; e^+e^- experiment.

PACS numbers: 13.25.Gv, 12.38.Qk, 14.40.Gx

I. INTRODUCTION

The study of the charmonium has been revived due to large data samples collected by CLEOC and BESII as well as by the B -factories. A prominent physics which has drawn interest for more than two decades is the very small branching fractions of $\rho\pi$ and other vector-pseudoscalar modes in ψ' decays compared with their large branching fractions in J/ψ decays. One proposal to solve this puzzle is the $2S$ - $1D$ states mixing scenario [1] which predicts enhanced rate of $\rho\pi$ mode in ψ'' decays. This scenario is extended to other decay modes besides $\rho\pi$, it foresees possible large partial widths for the light hadron modes in ψ'' decays [2, 3].

Recently, CLEOC and BESII reported the search for various light hadron decays of the ψ'' [4, 5, 6]. These experiments produce the ψ'' in e^+e^- collision so the radiative correction must be taken into account in the data analysis. Another feature of the data analysis of the resonances produced in e^+e^- collision is the need to consider the non-resonance continuum amplitude. For example, in the $e^+e^- \rightarrow \rho\pi$ data collected at the ψ'' mass, if the $2S$ - $1D$ mixing scenario gives correct $\mathcal{B}(\psi'' \rightarrow \rho\pi)$, then the non-resonance continuum amplitude is comparable to the ψ'' decay amplitude, the measured cross section is the result of the interference of the two [7]. For the narrow resonances like J/ψ , ψ' , $\Upsilon(1S)$, $\Upsilon(2S)$, and $\Upsilon(3S)$, the energy spread of the e^+e^- colliders must also be considered. But in this work, we concentrate on the wide resonances like ψ'' , of which the width is much wider than the finite energy spread of the e^+e^- colliders, so the energy spread does not change the observed cross section in any significant way. In this paper, we pay special attention to the circumstance that the interference between the amplitudes of the resonance and continuum has substantial contribution, particularly the circumstance that such interference is destructive. We present the characteristic features of the radiative correction under such circumstance. In the forthcoming sections, we begin with the amplitudes for the observed processes in e^+e^- experiments and the parametrization of them. Then we present the general properties of radiative correction. Next we turn to the Monte Carlo simulation. We discuss the invariant mass distribution of the final hadron systems for

the continuum process and for the pure resonance process, as well as for the circumstance in which both the resonance and continuum amplitudes exist and there is significant interference effect between them. Finally, we propose a possible scheme to verify the destructive interference with the data collected at the energy of the ψ'' mass for a detector with the energy-momentum resolution of $(1 \sim 2)\%$.

Avoiding complexity but without losing generality, we restrict our discussions on two situations in which the data are collected either off resonance at continuum, or at the energy of the resonance mass. For the experimental setting in which ψ'' is scanned, the technique details are more complicated. We shall leave its study to a future work. Through out the paper, the resonance ψ'' is taken as an example, but the analysis can be easily extended to other resonances with their width to mass ratios comparable to the energy-momentum resolution of the detector.

II. THREE AMPLITUDES IN e^+e^- EXPERIMENTS

The OZI suppressed decays of the ψ'' into light hadrons are via strong and electromagnetic interactions. In general, the cross section of e^+e^- to a certain final state at the resonance is expressed in the Born order by

$$\sigma_B(s) = \frac{4\pi s \alpha^2}{3} |a_{3g}(s) + a_\gamma(s)|^2 \mathcal{P}(s). \quad (1)$$

In the above equation, \sqrt{s} is the center-of-mass (C.M.) energy of e^+e^- , α is the QED fine structure constant, $a_{3g}(s)$ and $a_\gamma(s)$ denote the amplitudes in which the resonance decays via strong and electromagnetic interactions respectively, $\mathcal{P}(s)$ is the phase space factor for the final states. However, in e^+e^- colliding experiments, the continuum process

$$e^+e^- \rightarrow \gamma^* \rightarrow \text{hadrons}$$

may produce the same final hadronic states as the resonance decays do. We denote its amplitude by a_c , then the cross section becomes [8, 9]

$$\sigma_B(s) = \frac{4\pi s \alpha^2}{3} |a_{3g}(s) + a_\gamma(s) + a_c(s)|^2 \mathcal{P}(s). \quad (2)$$

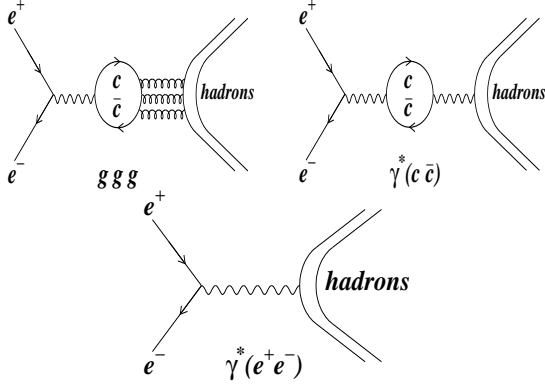


FIG. 1: The three classes of diagrams of $e^+e^- \rightarrow \text{light hadrons}$ at charmonium resonance. The charmonium state is represented by a charm quark loop.

So what truly contribute to the experimentally measured cross section are three classes of diagrams, *i.e.* the strong interaction presumably through three-gluon annihilation, the electromagnetic interaction through the annihilation of $c\bar{c}$ pair into a virtual photon, and the one-photon continuum process, as illustrated in Fig. 1, where the charm loops stand for the charmonium state. To analyze the experimental results, we must take these three amplitudes into account.

For an exclusive mode, a_c can be expressed by

$$a_c(s) = \frac{\mathcal{F}(s)}{s}, \quad (3)$$

where $\mathcal{F}(s)$ is the electromagnetic form factor which may have a dimension depending on the final states, here we define $\mathcal{F}(s)\mathcal{P}(s)$ to be dimensionless. We adopt the convention that a_c is real. Since a_γ is due to the resonance, it is expressed in the Breit-Wigner form

$$a_\gamma(s) = \frac{3\Gamma_{ee}\mathcal{F}(s)/(\alpha\sqrt{s})}{s - M^2 + iM\Gamma_t}, \quad (4)$$

where M and Γ_t are the mass and the total width of the resonance, Γ_{ee} is its partial width to e^+e^- . As a_{3g} is also due to the resonance decays, it can be parametrized relative to a_γ by a complex factor

$$\mathcal{C} \equiv |a_{3g}/a_\gamma|e^{i\phi}, \quad (5)$$

as

$$a_{3g}(s) = \mathcal{C} \cdot \frac{3\Gamma_{ee}\mathcal{F}(s)/(\alpha\sqrt{s})}{s - M^2 + iM\Gamma_t}. \quad (6)$$

Neglecting double OZI suppressed processes, the amplitudes of ψ'' decays into pairs of vector-pseudoscalar mesons (VP) are parametrized in terms of three parameters: the strong amplitude g , the electromagnetic amplitude e and the $SU(3)$ symmetry breaking factor $(1 - s_g)$ [10, 11]. These are listed in Table I for some of the measured decay modes together with the measured values by CLEOc [4] and BESII [5, 6]. Similar parametrization also applies to other OZI suppressed

two-body decays which conserve the generalized C-parity by appropriate change of labelling [10]. As for the decays to pairs of pseudoscalar-pseudoscalar mesons (PP) which violate the generalized C-parity, the amplitudes are parametrized in terms of two parameters: the electromagnetic amplitude E and strong $SU(3)$ breaking amplitude \mathcal{M} [10, 11]. These are listed in Table II, together with the BESII and CLEOc measurements [12, 13]. Similar parametrization can be extended to pairs of vector-vector mesons (VV). The amplitudes a_{3g} and a_γ can be expressed in terms of this parametrization scheme. For example, for $\rho\pi$ mode, $a_{3g} = g$, $a_\gamma = e$, $|\mathcal{C}| = |g/e|$; for $K^{*0}\bar{K}^0$, $a_{3g} = g(1 - s_g)$, $a_\gamma = -2e$, $|\mathcal{C}| = |g(1 - s_g)/(2e)|$; while for K^+K^- , $a_{3g} = \frac{\sqrt{3}}{2}\mathcal{M}$, $a_\gamma = E$, $|\mathcal{C}| = \frac{\sqrt{3}}{2}|\mathcal{M}/E|$. For VP final states, and other final states conserving the generalized C-parity, define

$$\theta_g = \arg\left(\frac{g}{e}\right),$$

while for PP and VV final states, define

$$\theta_g = \arg\left(\frac{\mathcal{M}}{E}\right),$$

we have $\phi = \theta_g$ if in Table I the sign between g and e is positive; and $\phi = \theta_g + 180^\circ$ if the sign between g and e is negative; while $\phi = \theta_g$ for K^+K^- in Table II. To include a_c in the formula, simply replace a_γ with $(a_\gamma + a_c)$.

If both the strong and electromagnetic interactions exist, the partial width of $\psi'' \rightarrow f$ is calculated by

$$\Gamma_f = \Gamma_{ee}|\mathcal{F}(s)|^2 \cdot |1 + \mathcal{C}|^2 \mathcal{P}(s). \quad (7)$$

If the decay to the final state only goes via electromagnetic interaction, then

$$\Gamma_f = \Gamma_{ee}|\mathcal{F}(s)|^2 \cdot \mathcal{P}(s). \quad (8)$$

As for the decay to $K_S^0 K_L^0$ mode which only goes via strong interaction (here we assume that there is no excited ϕ states in the vicinity), $\mathcal{F}(s) = 0$ since this mode does not couple to a virtual photon. Nevertheless, according to the parametrization in Table II, the decay modes K^+K^- and $K_S^0 K_L^0$ have the same strong decay amplitude, while $\pi^+\pi^-$ and K^+K^- have the same electromagnetic decay amplitude, which is consistent with the recently measured data listed in Table II within the experimental errors [13]. Under such assumption, $|\mathcal{C}|$ can be determined by the equation

$$\Gamma_{K_S^0 K_L^0} = \Gamma_{ee}|\mathcal{F}_{\pi^+\pi^-}(s)|^2 \cdot |\mathcal{C}|^2 \mathcal{P}(s). \quad (9)$$

Then with the measurement of K^+K^- mode, ϕ is obtained.

If the data is taken at the energy of the ψ'' mass, *i.e.* $s = M^2$, from Eq. (4) we see that a_γ has a phase of -90° relative to a_c . So there is no interference between a_c and a_γ . For the decay modes which go only via electromagnetic interaction, *e.g.* $\omega\pi^0$, $\rho\eta$, $\rho\eta'$ and $\pi^+\pi^-$, the

TABLE I: The experimental results from CLEOc [4] and BESII [5, 6] on ψ'' decays into VP modes and $b_1\pi$. Also listed is the parametrization of their amplitudes. Neglecting double OZI suppressed processes, the amplitudes of ψ'' decays into VP final states are parametrized by three terms: the strong amplitude g , the electromagnetic amplitude e and the SU(3) breaking factor $(1 - s_g)$ [10, 11]. Similar parametrization can be extended to other OZI suppressed two-body decays which conserve the generalized C-parity by appropriate change of labelling. The physical states η and η' are expressed by their quark components as $|\eta\rangle = X_{\eta}\frac{1}{2}|u\bar{u} + d\bar{d}\rangle + Y_{\eta}|s\bar{s}\rangle$ and $|\eta'\rangle = X_{\eta'}\frac{1}{2}|u\bar{u} + d\bar{d}\rangle + Y_{\eta'}|s\bar{s}\rangle$.

Channel	Amplitude	CLEOc		BESII	
		$\sigma(3.671 \text{ GeV})$ [pb]	$\sigma(3.773 \text{ GeV})$ [pb]	$\sigma(3.650 \text{ GeV})$ [pb]	$\sigma(3.773 \text{ GeV})$ [pb]
VP					
$\rho^+\pi^-, \rho^-\pi^0, \rho^-\pi^+$	$g + e$	$8.0^{+1.7}_{-1.4} \pm 0.9$	$4.4 \pm 0.3 \pm 0.5$	< 25	< 6.0
$\omega\pi^0$	$3e$	$15.2^{+2.8}_{-2.4} \pm 1.5$	$14.6 \pm 0.6 \pm 1.5$	$24.2^{+11}_{-9} \pm 4.3$	$10.7^{+5.0}_{-4.1} \pm 1.7$
$\phi\pi^0$	0	< 2.2	< 0.2		
$\rho\eta$	$3eX_{\eta}$	$10.0^{+2.2}_{-1.9} \pm 1.0$	$10.3 \pm 0.5 \pm 1.0$	$8.1^{+7.4}_{-4.9} \pm 1.1$	$7.8^{+4.4}_{-3.5} \pm 0.08$
$\omega\eta$	$(g + e)X_{\eta}$	$2.3^{+1.8}_{-1.1} \pm 0.5$	$0.4^{+0.2}_{-0.2} \pm 0.1$		
$\phi\eta$	$[g(1 - 2s_g) - 2e]Y_{\eta}$	$2.1^{+1.9}_{-1.2} \pm 0.2$	$4.5 \pm 0.5 \pm 0.5$		
$\rho\eta'$	$3eX_{\eta'}$	$2.1^{+4.7}_{-1.6} \pm 0.2$	$3.8^{+0.9}_{-0.8} \pm 0.4$	< 89	< 28
$\omega\eta'$	$(g + e)X_{\eta'}$	< 17.1	$0.6^{+0.8}_{-0.3} \pm 0.6$		
$\phi\eta'$	$[g(1 - 2s_g) - 2e]Y_{\eta'}$	< 12.6	$2.5^{+1.5}_{-1.1} \pm 0.4$		
$K^{*0}\bar{K}^0, \bar{K}^{*0}K^0$	$g(1 - s_g) - 2e$	$23.5^{+4.6}_{-3.9} \pm 3.1$	$23.5 \pm 1.1 \pm 3.1$		
$K^{*+}K^-, K^{*-}K^+$	$g(1 - s_g) + e$	$1.0^{+1.1}_{-0.7} \pm 0.5$	< 0.6		
AP					
$b_1\pi$	$g + e$	$7.9^{+3.1}_{-2.5} \pm 1.8$	$6.3 \pm 0.7 \pm 1.5$		

TABLE II: The measured $\pi^+\pi^-, K^+K^-$ cross sections at $E_{cm} = 3.671 \text{ GeV}$ by CLEOc[13] and the upper limit of $K_S K_L$ cross sections at $E_{cm} = 3.65 \text{ GeV}$ by BES [12]. Also listed is the parametrization of ψ'' decays into PP final states. These amplitudes are parametrized in terms of electromagnetic amplitude E and strong SU(3) breaking amplitude \mathcal{M} [10, 11]. Similar parametrization can be applied to VV final states.

final state	$\sigma(3.671 \text{ GeV})$	amplitude
$\pi^+\pi^-$	$9.0 \pm 1.8 \pm 1.3 \text{ pb}$	E
K^+K^-	$5.7 \pm 0.7 \pm 0.3 \text{ pb}$	$E + \frac{\sqrt{3}}{2}\mathcal{M}$
$K_S^0 K_L^0$ ($< 5.9 \text{ pb}$ at 90% C.L. at 3.65 GeV)		$\frac{\sqrt{3}}{2}\mathcal{M}$

interference between the resonance and continuum can be neglected. (Under such circumstance, the interference is still non-vanishing due to two reasons: first, for the practical reason in the experiments, the data is usually taken at where the maximum inclusive hadron cross section is, which in general does not coincide with the mass of the resonance [14]; second, even if the data is collected at the energy of the resonance mass, the interference is non-vanishing because of radiative correction. This will be proved later on in this paper. For the narrow resonances with widths smaller than the energy spread of the e^+e^- colliders, the smearing of the C.M. energy also results in a non-vanishing interference term. But these are beyond the concern for the accuracy of current experiments.) Under such circumstance, in the data analysis we simply subtract the continuum cross section from the cross section measured on top of the resonance to get the resonance cross section. The ratio of the resonance cross section of a particular final state to the total resonance

cross section gives the branching fraction of this mode. For the ψ'' , a_{γ} is very small compared to a_c . This is seen that if $s = M^2$,

$$|a_{\gamma}(M_{\psi''}^2)/a_c(M_{\psi''}^2)| = \frac{3}{\alpha}\mathcal{B}(\psi'' \rightarrow e^+e^-).$$

With the measured value of $\mathcal{B}(\psi'' \rightarrow e^+e^-) = (1.12 \pm 0.17) \times 10^{-5}$ [15],

$$|a_{\gamma}(M_{\psi''}^2)/a_c(M_{\psi''}^2)| \approx 4.6 \times 10^{-3}.$$

So a_{γ} can be neglected. For those modes which only go via electromagnetic interaction, the measured cross sections at the ψ'' mass almost entirely come from the non-resonance continuum amplitude a_c . This is demonstrated by the experimental results on $\omega\pi^0$, $\rho\eta$, and $\rho\eta'$ modes in Table I where their cross sections measured at the ψ'' peak are consistent with the ones measured off the resonance within experimental errors with the later scaled for s dependence.

But for other final states which have contributions from a_{3g} besides a_{γ} , there could be interference between a_{3g} and a_c as well as between a_{3g} and a_{γ} . Since for the ψ'' , a_{γ} is very small compared to a_c , so only the interference between a_{3g} and a_c could be important. Based on the analysis of the experimental data, we have suggested that the phase θ_g is universally -90° in quarkonium decays [16, 17]. Since at the energy of resonance mass, the phase of a_{γ} is -90° relative to a_c , so the relative phase between a_{3g} and a_c is either 180° or 0° , depending on whether the relative sign between g and e in Table I, or between \mathcal{M} and E in Table II is plus or minus. The interference between a_{3g} and a_c is destructive for the final states $\rho\pi$, $\omega\eta$, $\omega\eta'$, $K^{*+}K^- + c.c.$, $b_1\pi$, and K^+K^- , but constructive for $\phi\eta$, $\phi\eta'$, and $K^{*0}\bar{K}^0 + c.c.$

Destructive interference between a_{3g} and a_c means that the observed cross section at the energy of the resonance mass can be smaller than the continuum cross section. The experimental results on $\rho\pi$ and $\omega\eta$ modes in Table I demonstrate this interference pattern.

III. RADIATIVELY CORRECTED CROSS SECTION

The actual description of e^+e^- to a final hadronic state through the annihilation of a virtual photon must incorporate radiative correction. Such correction mainly comes from the initial state radiation, and for the hadronic final state, the final state radiation usually can

be neglected [18].

The integrated cross section by e^+e^- collision incorporating radiative correction is expressed by [19]

$$\sigma_{r.c.}(s) = \int_0^{1-s_m/s} dx F(x, s) \sigma_B(s(1-x)) \quad (10)$$

where $\sigma_B(s)$ is the Born order cross section by Eq. (2), and in the upper limit of the integration $\sqrt{s_m}$ is the cut-off invariant mass of the final state hadron system after losing energy to photon emission. $F(x, s)$ is calculated to an accuracy of 0.1% in Ref. [19]:

$$\begin{aligned} F(x, s) = & \beta x^{\beta-1} \left[1 + \frac{3}{4}\beta + \frac{\alpha}{\pi} \left(\frac{\pi^2}{3} - \frac{1}{2} \right) + \beta^2 \left(\frac{9}{32} - \frac{\pi^2}{12} \right) \right] - \beta \left(1 - \frac{x}{2} \right) \\ & + \frac{1}{8}\beta^2 \left[4(2-x) \ln \frac{1}{x} - \frac{1+3(1-x)^2}{x} \ln(1-x) - 6+x \right], \end{aligned} \quad (11)$$

with

$$\beta = \frac{2\alpha}{\pi} \left(\ln \frac{s}{m_e^2} - 1 \right). \quad (12)$$

In the above equations, m_e is the mass of the electron. Here the expression $F(x, s)$ includes the bremsstrahlung of an e^+e^- pair from the initial e^+e^- state. For $x \sim 0$, $x\sqrt{s}/2$ is approximately equal to the energy carried away by the radiated photons. But for $x \sim 1$, this meaning is

not valid in the α^2 order. The effects of vacuum polarization are not included explicitly in Eq. (10). Here we follow the convention that for hadronic final state, the vacuum polarization by leptons and hadrons, including vector-meson resonances, is taken into account in the form factor $\mathcal{F}(s)$ [20].

In Eq. (10), $F(x, s)$ is positive definite. If $s = M^2$, for pure electromagnetic processes, the interference term between a_γ and a_c in $\sigma_B(s(1-x))$, i.e.

$$\begin{aligned} 2\Re[a_\gamma(s(1-x))a_c(s(1-x))] &= 2\Re \left[\frac{\mathcal{F}(s(1-x))}{s(1-x)} \cdot \frac{3\Gamma_{ee}\mathcal{F}(s(1-x))/(\alpha\sqrt{s(1-x)})}{s(1-x) - M^2 + iM\Gamma_t} \right] \\ &= 2[s(1-x) - M^2] \cdot \frac{3|\mathcal{F}(s(1-x))|^2\Gamma_{ee}}{\alpha[s(1-x)]^{3/2}[(s(1-x) - M^2)^2 + M^2\Gamma_t^2]}, \end{aligned} \quad (13)$$

vanishes only at $x = 0$, but it is negative elsewhere in the integration interval from 0 to $1 - s_m/s$. So even in the pure electromagnetic processes, with radiative correction, the interference term gets a negative value.

In Eqs. (3), (4) and (6), the form factor $\mathcal{F}(s)$ is adopted to describe the hadronic interaction. Both the Monte Carlo simulation and the calculation of the radiatively corrected cross section require the knowledge of the form factor in the energy range from \sqrt{s} down to $\sqrt{s_m}$. In principle, $\sqrt{s_m}$ can be as low as the production threshold.

But this requires the input values of the form factor from \sqrt{s} to the production threshold. In Eq. (10), $F(x, s)$ has been calculated to an accuracy of 0.1% by QED, but for virtually all the hadronic final states, we have neither the theoretical models nor sufficient experimental data to describe the form factors to such high precision. To reduce the systematic uncertainty from the Monte Carlo simulation, one strategy is to take the value of s_m as close to s as possible for the actual event selection criteria, i.e. we generate the event sample with s_m just lower than

that which are to be selected. In this way, we need only to describe the form factor precisely from \sqrt{s} down to a much higher $\sqrt{s_m}$, instead of to the production threshold.

The variation of the form factor in a small energy interval usually can well be approximated by

$$\mathcal{F}(s') = \mathcal{F}(s) \left(\frac{s}{s'} \right)^k, \quad (14)$$

with k either derived from theoretical models, or obtained from fitting the experimental data at nearby energy. Of course one may use a more complicated function other than Eq. (14) for the approximation.

IV. MONTE CARLO SIMULATION

A. Soft and hard photon events

In realization of Monte Carlo simulation, an auxiliary parameter x_0 is introduced to separate the integration interval of Eq. (10) into two parts, $(0, x_0)$ and $(x_0, 1 - s_m/s)$, with x_0 a small but nonzero value:

$$\sigma_{soft}(s) = \int_0^{x_0} dx F(x, s) \sigma_B(s(1-x)) \quad (15)$$

and

$$\sigma_{hard}(s) = \int_{x_0}^{1-s_m/s} dx F(x, s) \sigma_B(s(1-x)) \quad (16)$$

In the above two equations, all functions and variables have the same meaning as in Eq. (10). We have

$$\sigma_{r.c.}(s) = \sigma_{soft}(s) + \sigma_{hard}(s).$$

The two terms in the above expression are usually called soft photon and hard photon cross sections respectively. The Monte Carlo program generates the soft photon events and hard photon events according to their proportions in the total cross section. In a soft photon event, the four-momentum of the radiated photons are neglected, and the photons are not generated. Experimentally, this means that in the soft photon events, the photons can not be detected. Since in Eq. (15), x_0 is small, so $x_0\sqrt{s}/2$ can be identified as the maximum energy carried away by the undetected photons. This requires that $x_0\sqrt{s}/2$ must be smaller than the minimum energy of the photon which can be detected in the experiment. In a soft photon event, the energy-momentum is conserved between the incoming e^+e^- pair and the final state hadron system, so x_0 must also be smaller than the energy-momentum resolution of the detector. Usually x_0 is assigned a nonzero value smaller than 0.01. The outcome of the Monte Carlo simulation does not depend on x_0 . In a hard photon event, the four-momentum of the radiated photons are generated, and the energy-momentum is conserved with the inclusion of these photons.

The differential cross sections with the emission of photons for exclusive hadronic processes are calculated in Refs. [21, 22], the calculation of Ref. [23] can also be used to generate the hard photon events while the generation of soft photon events is identical to the generation of events at Born order. (The inclusive process is treated somewhat differently in Ref. [24].) The authors of these references also provide Monte Carlo programs based on their calculations. The program based on the calculation in Ref. [21], BABAYAGA, generates $\pi^+\pi^-$ events; the program based on Ref. [22], MCGPJ with the current version, generates $\pi^+\pi^-$, K^+K^- , and $K_S K_L$ events; while the program based on Ref. [23] generates hard photon events for $\pi^+\pi^-$, $\pi^+\pi^-\pi^0$, $\pi^+\pi^-\pi^+\pi^-$, and $\pi^+\pi^-\pi^0\pi^0$ processes. These programs achieve the precision of $(0.1 \sim 0.2)\%$.

In order to generate events with the presence of both the ψ'' resonance and continuum, some replacements are to be made in the fore-mentioned programs. The Born order cross section by Eq. (2) must be substituted to generate the correct distribution of the invariant mass of the final state hadron systems. Although the original programs only generate a few hadronic final states, the programs based on Refs. [22, 23] are written in the form that more final states can be added in a straightforward way. To do this, one need to put the corresponding hadronic tensor $H_{\mu\nu}$ into the program, where

$$H_{\mu\nu} = \mathcal{H}_\mu \times \mathcal{H}_\nu^*, \quad (17)$$

with \mathcal{H}_μ the current of virtual photon transition to the final hadron state f . For reference we include its forms for some final hadronic states in the appendix.

B. Distribution of invariant mass of hadrons

The distribution of the invariant mass of the final hadron system M_{inv} is very different between resonance and continuum. More profound distinctive feature is in the circumstance that there is interference, particularly destructive one, between the resonance and continuum. In this section, we discuss this distribution.

1. Resonance

If the final state does not couple to a virtual photon, e.g. $K_S^0 K_L^0$, then in Eq. (2), there is only the a_{3g} term, the Born order cross section is expressed by the Breit-Wigner formula:

$$\sigma_{res}(s) = \frac{12\pi\Gamma_{ee}\Gamma_f}{(s - M^2)^2 + M^2\Gamma_t^2}, \quad (18)$$

where Γ_f is the partial width to the final state f .

For narrow resonances, by narrow we mean $\Gamma_t/M \ll x_0$, Eq. (18) behaves almost like a δ function. If the data is taken at the energy of the resonance mass, i.e. $s = M^2$,

in Eq. (18), $\sigma_{res}(s(1-x))$ is very large at $x = 0$ and very small elsewhere. So in Eq. (10), the contribution of $\sigma_B(s(1-x))$ to the radiatively corrected cross section comes solely from a small interval around $x = 0$. Substitute $\sigma_{res}(s(1-x))$ for $\sigma_B(s(1-x))$ in Eqs. (15) and (16), σ_{soft} is nonzero while σ_{hard} virtually vanishes due to their integration intervals respectively. This means that in the Monte Carlo simulation of a narrow resonance, only the soft photon events are generated. The sole effect of the radiative correction is the reduction of its height. This will be discussed later in this paper.

The resonance ψ'' is not very narrow in this sense. If we take $x_0 = 0.01$ and $s_m = 0.8M^2$, soft photon events are 98.6% of the total.

2. Non-resonance continuum

For continuum process, there is a considerable hard photon cross section. Take an example of VP final states,

$$\begin{aligned}\sigma_B(s(1-x)) &= \frac{4\pi s(1-x)\alpha^2}{3} |a_c(s(1-x)) + a_{3g}(s(1-x)) + a_\gamma(s(1-x))|^2 \mathcal{P}(s(1-x)) \\ &= \frac{4}{3}\pi s(1-x)\alpha^2 |\mathcal{F}(s(1-x))|^2 \mathcal{P}(s(1-x)) \times \left| \frac{1}{s(1-x)} + (\mathcal{C} + 1) \frac{3\Gamma_{ee}/(\alpha\sqrt{s(1-x)})}{s(1-x) - M^2 + iM\Gamma_t} \right|^2.\end{aligned}\quad (19)$$

We pay special attention to the destructive interference and take as an extreme example the circumstance that a_{3g} and a_c almost cancel to each other in the Born order. This happens if

$$|\mathcal{C}| \approx \frac{\alpha\Gamma_t}{3\Gamma_{ee}}, \quad \phi = -90^\circ. \quad (20)$$

Under such circumstance, the partial width of this final state is expressed by

$$\Gamma_f \approx \frac{M^2\Gamma_t^2}{12\pi\Gamma_{ee}} \sigma_{con}(M^2), \quad (21)$$

where $\sigma_{con}(M^2)$, scaled for s dependence to $s = M^2$, is the Born order cross section for the non-resonance continuum.

To calculate the proportion of soft and hard photon events, Eq. (19) is to be substituted into Eqs. (15) and (16) respectively. Notice that these two equations only differ by their integration intervals. For the discussions on the ψ'' in this work, we take $x_0 = 0.01$ which is greater than Γ_t/M . If the resonance amplitude satisfies Eq. (20), then for Eq. (15), in the integration interval $(0, x_0)$, there is almost complete cancellation between the two terms of $\sigma_B(s(1-x))$; while for Eq. (16), in the integration interval $(x_0, 1 - s_m/s)$, the magnitude of the resonance which

with $x_0 = 0.01$ and $s_m = 0.8s$, and assuming that the form factor varies as a function of energy according to $1/s$ ($k = 1$ in Eq. (14)), in the simulation the hard photon events are 22% of the total.

3. Interference between resonance and continuum

If both the resonance and continuum amplitudes exist, the Born order cross section is obtained from Eq. (2) with a_c , a_γ and a_{3g} by Eqs. (3), (4), and (6).

is the second term of $\sigma_B(s(1-x))$, virtually vanishes. This means that the resonance and its interference with continuum affect mainly the soft photon cross section; while the hard photon cross section is predominately due to a_c . In this way, the interference changes the proportions of the soft and hard photon events as well as the total radiatively corrected cross section. The destructive interference between resonance and non-resonance continuum reduces the soft photon cross section, which means a smaller proportion of soft photon events.

To illustrate the above discussion quantitatively, we take the example that the resonance amplitude satisfies Eq. (20). Under such circumstance, the proportion of the soft photon events is 15% for $x_0 = 0.01$ and $s_m = 0.8s$. (This is not the lowest possible proportion of the soft photon events. With $\phi = -90^\circ$, the complete cancellation happens only between a_{3g} and a_c . There is still a small but non-vanishing a_γ left. If a_{3g} cancels out not only a_c , but also a_γ , the proportion of soft photon events can be even smaller.) This means that for a detector with energy-momentum resolution $x_0/2 = 0.5\%$, among the data taken at non-resonance continuum, 78% of the events have invariant mass equal to the C.M. energy of the incoming e^+e^- ; while among the data taken at the ψ'' mass, we may find that the majority of the events (85%) have invariant mass smaller than the C.M. en-

ergy of the incoming e^+e^- . If this happens, it indicates destructive interference between the resonance and non-resonance continuum amplitudes.

Fig. 2 shows the probability density as a function of the squared invariant mass of the final hadron system M_{inv}^2 . For continuum, as well as for no interference or constructive interference between the resonance and continuum cases, the maximum probability density occurs (actually diverges) at $M_{inv}^2 = s$, which corresponds to $E_\gamma \rightarrow 0$ with E_γ the energy of the emitted photons; but if the destructive interference between a_{3g} and a_c exists, and it leads to almost complete cancellation of the two amplitudes, the probability density may have a minimum point near $M_{inv}^2 = s$.

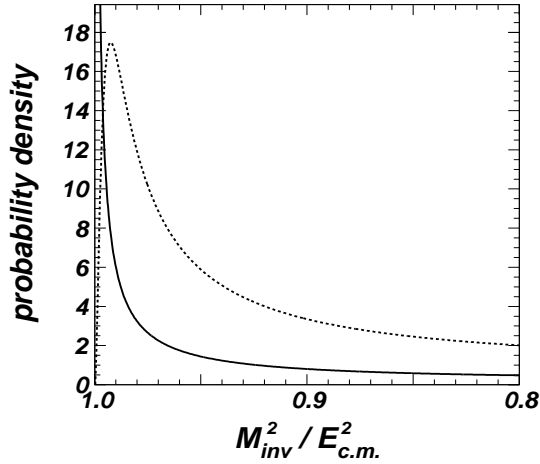


FIG. 2: The distribution of the probability density as a function of M_{inv}^2/s with M_{inv} the invariant mass for a VP final state. The solid line is for continuum. The dashed line is an example of destructive interference between a_{3g} and a_c with the two amplitudes satisfying Eq. (20). The probability is normalized to $\sigma_{r.c.}(M_{\psi''}^2)$ with $s_m = 0.8s$.

In the circumstance that at $s = M^2$, the three terms in Eq. (2) completely cancel, i.e. $a_{3g} + a_\gamma + a_c = 0$, so the Born order cross section vanishes, the radiatively corrected cross section $\sigma_{r.c.}(s)$ still gets a nonzero value, as long as $s_m < s$. This is because that in Eq. (10), $F(x, s)$ is a positive definite function, while $\sigma_B(s(1-x))$ vanishes only at $x = 0$, but remains positive definite elsewhere in the integration interval. This leads to the phenomena in e^+e^- experiments: a detector with finite energy-momentum resolution always observes a non-vanishing cross section, even if the Born order cross section vanishes due to destructive interference between the resonance and continuum.

C. The calculated efficiency

According to Eq. (10), $\sigma_{r.c.}$ is a function of s_m as well as s . For the reason which we discussed in Sec. III, in the Monte Carlo simulation, usually we generate events to a

cut-off invariant mass $\sqrt{s_m}$, so the calculated efficiency ϵ is also a function of s_m .

If the observed number of event is denoted as N , corresponding integrated luminosity is denoted as \mathcal{L} , then we have

$$N = \mathcal{L} \cdot \sigma_{r.c.}(s, s_m) \cdot \epsilon(s_m),$$

here and in the following discussions, we explicitly indicate the dependence of $\sigma_{r.c.}$ and ϵ on s_m . The above equation can also be expressed as

$$\frac{N}{\mathcal{L}} = \sigma_{r.c.}(s, s_m) \cdot \epsilon(s_m). \quad (22)$$

The left side of the above expression is an experimentally measured quantity. The product $\sigma_{r.c.}(s, s_m) \cdot \epsilon(s_m)$ does not depend on s_m .

Very often, the experimental results are presented in terms of Born order cross section, particularly the off resonance continuum cross section. For the data taken off the resonance, we measure the electromagnetic form factor of the final state, which is simply related to the Born order cross section. A so-called radiative correction factor is introduced as

$$f_{ISR}(s, s_m) = \frac{\sigma_{r.c.}(s, s_m)}{\sigma_B(s)}. \quad (23)$$

Here if the form factor takes the form of Eq. (14), then $f_{ISR}(s, s_m)$ can be calculated. It does not depend on $\mathcal{F}(s)$, although it still depends on k in Eq. (14). With Eqs. (22) and (23), we have

$$\sigma_{Born}(s) = \frac{\sigma_{r.c.}(s, s_m)}{f_{ISR}(s, s_m)} = \frac{N}{\mathcal{L} \cdot \epsilon(s_m) \cdot f_{ISR}(s, s_m)}.$$

In the denominator, the product of $\epsilon(s_m) \cdot f_{ISR}(s, s_m)$ cancels out the dependence on s_m .

The interference between the resonance and continuum amplitudes may change the factor f_{ISR} in a profound way. For non-resonance continuum, with \sqrt{s} well above the production threshold, if the form factor goes down rapidly as s increases (e.g. $k \geq 1$ in Eq. (14)), as s_m approaches the threshold, f_{ISR} is usually greater than 1; but if s_m is taken close to s , then f_{ISR} can always be smaller than 1, since as $s_m \rightarrow s$, $\sigma_{r.c.}(s, s_m) \rightarrow 0$. For a resonance, f_{ISR} does not depend on k . It is roughly approximated by [14]

$$f_{ISR} \approx \left(\frac{\Gamma_t}{M}\right)^\beta \left[1 + \frac{3}{4}\beta + \frac{\alpha}{\pi} \left(\frac{\pi^2}{3} - \frac{1}{2}\right) + \beta^2 \left(\frac{9}{32} - \frac{\pi^2}{12}\right)\right] \quad (24)$$

Here β is given by Eq. (12). If $\Gamma_t \ll M$, the value of this expression is less than 1. It means that the initial state radiation reduces the height of the resonance. If there is significant interference between the resonance and continuum, f_{ISR} may take any value between the order of 1 to infinity. It becomes infinity in the circumstance that $\sigma_B(s)$ vanishes due to destructive interference

between the resonance and continuum. As discussed in Sec. IV B 3, $\sigma_{r.c.}(s, s_m)$ still gets a nonzero value in this circumstance.

For illustrative purpose, here we take an example that in the Monte Carlo simulation of e^+e^- collision at $\sqrt{s} = M_{\psi''}$, the VP final state events with the cut-off invariant mass of $0.9M_{\psi''}$ are generated, and the form factor varies as a function of the energy according to $1/s$, while in the data selection, the invariant mass of the final VP particles is required to be greater than $98\%\sqrt{s}$. Under these conditions, for the continuum cross section, 87.4% of the generated events survives and $f_{ISR} = 0.946$; for the ψ'' resonance, 99.9% of the generated events is left and $f_{ISR} = 0.716$; while for the destructive interference between a_{3g} and a_c which satisfies Eq. (20), only 49.0% of the generated events have invariant mass greater than $98\%M_{\psi''}$, but $f_{ISR} = 65.5$.

V. MEASUREMENT IN THE PRESENCE OF INTERFERENCE

The above discussions lead to a profound feature of the experimental measurement in the presence of interference between the resonance and non-resonance continuum: the complete determination of the branching fraction must come together with the determination of the phase between the resonance and continuum by scanned data around the resonance peak. The data must be taken at least at four energy points, because there are three quantities which must be determined simultaneously: $\mathcal{F}(M^2)$, $|\mathcal{C}|$ and ϕ . At the same time, the form of dependence of the observed cross section on $|\mathcal{C}|$ is quadric. Herein the non-resonance continuum amplitude or equivalently $\mathcal{F}(M^2)$ is determined by the data taken at continuum. In the treatment of the data taken around the resonance, if both strong and electromagnetic interactions exist, the Monte Carlo generator requires the input of $|\mathcal{C}|$ and ϕ , so the data analysis is an iterative process. The usual procedure is to fix ϕ , and varying $|\mathcal{C}|$, until the calculated efficiency $\epsilon(s_m)$ by the Monte Carlo and the radiatively corrected cross section $\sigma_{r.c.}(s, s_m)$ satisfy Eq. (22). Then the partial width is obtained by Eq. (7).

If the data are taken at two points, i.e. one at continuum off the resonance and the other one at the energy of the resonance mass, only a relation between $|\mathcal{C}|$ and ϕ can be obtained. The solution of $|\mathcal{C}|$ and ϕ is differentiated into two circumstances, depending on the relative magnitudes of the observed total cross section σ_t and continuum cross section σ_c . Here σ_c is the radiatively corrected cross section of the non-resonance continuum calculated with the form factor at the energy $\sqrt{s} = M_{\psi''}$. As in the Born order cross sections, if $\sigma_t > \sigma_c$, ϕ can take any value from -180° to 180° , and for each value of ϕ there is one and only one solution for $|\mathcal{C}|$; on the other hand, if $\sigma_t < \sigma_c$, ϕ is constrained within a range around -90° , in which every possible value of ϕ corresponds to two solutions of $|\mathcal{C}|$. A formal discussion is left into the appendix.

In such measurement, $|\mathcal{C}|$ is determined versus the phase ϕ in a two dimensional curve. The recommended way is to start from $\phi = -90^\circ$, since there is always at least one solution of $|\mathcal{C}|$. If the obtained σ_t is smaller than σ_c , the second solution must be searched. Then for the ϕ values greater and smaller than -90° , the solutions of $|\mathcal{C}|$ are found similarly. Thus the curve relating $|\mathcal{C}|$ with ϕ is obtained point by point.

Although $\sigma_{r.c.}(s, s_m)$ and $\epsilon(s_m)$ depend on $|\mathcal{C}|$ and ϕ , for different solutions of $|\mathcal{C}|$ and ϕ which fit the experimental data, $\sigma_{r.c.}(s, s_m)$ and $\epsilon(s_m)$ only depend on $|\mathcal{C}|$ and ϕ weakly. This can be understood by noticing that the efficiency can be expressed in terms of the efficiency for soft photon events $\epsilon_{soft}(x_0)$, and the one for hard photon events $\epsilon_{hard}(s_m)$. Apparently we have

$$\sigma_{r.c.}(s, s_m)\epsilon(s_m) = \sigma_{soft}(s, x_0)\epsilon_{soft}(x_0) + \sigma_{hard}(s, s_m)\epsilon_{hard}(s_m). \quad (25)$$

As discussed in Sec. IV B 3, if we take $x_0 > \Gamma_t/M$, the distribution of the hard photon events and the hard photon cross section are predominately due to a_c , so $\sigma_{hard}(s, s_m)$ and $\epsilon_{hard}(s_m)$ are almost independent of $|\mathcal{C}|$ and ϕ . As for the soft photon events, the distribution follows the Born order differential cross section, so $\epsilon_{soft}(x_0)$ does not depend on $|\mathcal{C}|$ and ϕ either. So in Eq. (25), for a rough approximation, only $\sigma_{soft}(s, x_0)$ depends on $|\mathcal{C}|$ and ϕ . The solutions of $|\mathcal{C}|$ and ϕ are to satisfy the equation

$$\frac{N}{\mathcal{L}} = \sigma_{soft}(s)\epsilon_{soft} + \sigma_{hard}(s, s_m)\epsilon_{hard}(s_m). \quad (26)$$

Here N/\mathcal{L} is given by the experiment, only $\sigma_{soft}(s, x_0)$ depends on $|\mathcal{C}|$ and ϕ , so $\sigma_{soft}(s, x_0)$ remains as a constant for any possible solution of $|\mathcal{C}|$ and ϕ which fit the data. Since $\sigma_{r.c.}(s, s_m) = \sigma_{soft}(s, x_0) + \sigma_{hard}(s, s_m)$, and $N/\mathcal{L} = \sigma_{r.c.}(s, s_m)\epsilon(s_m)$, $\sigma_{r.c.}(s, s_m)$ and $\epsilon(s_m)$ are almost constants as well. This property helps to find other solutions with different $|\mathcal{C}|$ and ϕ values once one of the solution is found. It also makes the iterative process converge very fast.

VI. VERIFY THE INTERFERENCE WITH THE DATA AT ψ''

The discussions in Sec. IV B leads to a scheme which could verify the destructive interference between ψ'' and non-resonance continuum with only the data at ψ'' peak. Modern detectors with a CsI(Tl) calorimeter and a magnetic field of 1 Tesla or more, like CLEOC and BESIII, measure the energy-momentum with resolution of 1%, which is comparable to the ratio $\Gamma_{\psi''}/M_{\psi''}$. In this scheme the invariant mass distribution of the hadrons is measured, and in the event selection, requirement of the invariant mass, M_{inv} , greater than a certain value, M_{cut} , is applied. For non-resonance continuum, as M_{cut} is loosed from $0.99\sqrt{s}$ to, e.g. $0.95\sqrt{s}$ or $0.90\sqrt{s}$, the number of events increases slowly; for no interference or constructive interference between the resonance and continuum, the number of events increases even slower; for

TABLE III: The variation of the cross section as a function of M_{cut} for the non-resonance continuum and the destructive interference between a_{3g} and a_c with the two amplitudes satisfying Eq. (20), taking the cross sections with $M_{cut} = 0.99\sqrt{s}$ as the unit.

M_{cut}/\sqrt{s}	destructive interference	continuum
0.99	1.00	1.00
0.98	1.61	1.06
0.97	2.00	1.09
0.96	2.30	1.12
0.95	2.53	1.14
0.90	3.33	1.21

pure resonance, the number of events does not increase at all; on the other hand, if the destructive interference leads to substantial cancellation between the resonance and continuum amplitudes, as M_{cut} is lowered, the number of events increases rapidly. Table III gives the the cross section as a function of M_{cut} , taking the cross section with $M_{cut} = 0.99\sqrt{s}$ as the unit. Listed cross sections are due to the non-resonance continuum and the destructive interference between a_{3g} and a_c with the amplitudes satisfying Eq. (20). It is assumed that the final state is VP and the form factor varies as a function of energy according to $1/s$. Fig. 3 shows the cross section as a function of M_{cut} for these two circumstances, normalized to the cross section with $M_{cut} = 0.99\sqrt{s}$. In Fig. 3 and Table III, we see that, as M_{cut} is loosed from $99\%\sqrt{s}$ to $90\%\sqrt{s}$, the cross section of the continuum increases by merely 21%; but for the destructive interference, it could increase by more than 3 times. In the experimental data, if the number of events increases rapidly as one lowers M_{cut} in event selection, it indicates destructive interference between ψ'' and continuum with the two amplitudes in comparable strength.

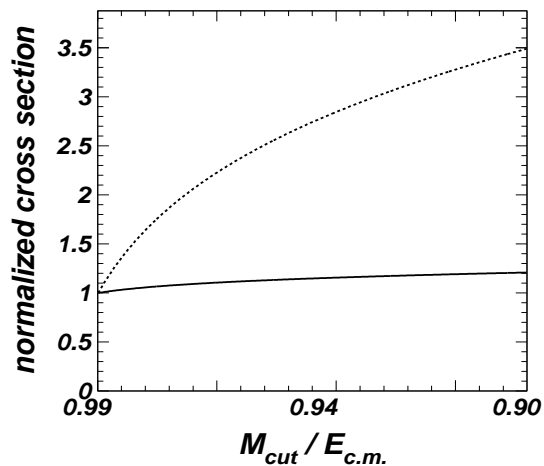


FIG. 3: The cross section as a function of M_{cut} normalized to the cross section with $M_{cut} = 0.99\sqrt{s}$. Solid line is for continuum. Dashed line is for destructive interference between a_{3g} and a_c with the two amplitudes satisfying Eq. (20).

To simulate the experimental situation, in Fig. 4 the interval of the invariant mass of the final state hadron system from 100% to 90% of the e^+e^- C.M. energy is divided into 20 bins, and the probabilities of the hadrons in the bins are plotted for the events at continuum and at the energy of ψ'' mass with the destructive interference between a_{3g} and a_c satisfying Eq. (20). Here off resonance at continuum, the events are highly concentrated in the last bin with $M_{inv}/E_{c.m.} = 100\%$; while for destructive interference, the events are distributed more flatly among the bins. If there is no interference or if the interference is constructive, the events are even more concentrated in the last bin than off resonance at continuum in the plot.

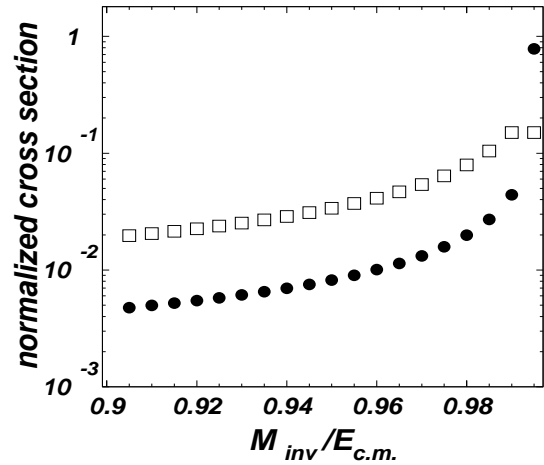


FIG. 4: The interval of the invariant mass of the final state hadron system from 100% to 90% of the e^+e^- C.M. energy is divided into 20 bins, the probabilities of the hadron event in each bin are plotted for continuum (dots) and for the ψ'' with the destructive interference between a_{3g} and a_c satisfying Eq. (20) (boxes).

This scheme requires the selected data sample be free from background contamination. The most important background comes from the radiative tail of the ψ' . For the data taken at the ψ'' peak, the radiative tail due to the ψ' has an invariant mass which is 97.8% of the e^+e^- C.M. energy. The radiative tail of the ψ' at the energy of the ψ'' mass has a total cross section of 2.6 nb, so this scheme is feasible for those decay modes like $\rho\pi$, $K^{*+}K^-$, and $\omega\eta$ with branching fractions in ψ' decays no more than the order of 10^{-5} [25, 26] since the background of these modes from radiative tail of the ψ' is at the order of 0.1 pb. But for those modes which have large branching fractions in ψ' decays, e.g. $b_1\pi$, the contribution of the ψ' tail must be considered carefully.

VII. SUMMARY

In this paper, we examined the radiative correction and Monte Carlo simulation for the measurement of ψ'' exclusive decays into light hadrons in e^+e^- experiments. We

draw special attention on the interference effect between the ψ'' resonance and non-resonance continuum amplitudes. We analyzed how the interference, particularly the destructive interference may change the invariant mass distribution of the final state hadrons. The discussions also lead to a possible scheme to verify the destructive interference using only the data taken at the energy of the ψ'' mass for the detectors with the energy-momentum resolution of $(1 \sim 2)\%$. We suggest this scheme be applied on decays such as $\omega\eta$, $\omega\eta'$, $K^{*+}K^-$, and $\rho\pi$ by future BESIII experiment.

APPENDIX A: THE HADRONIC CURRENT

The current of virtual photon transition to the final state f is defined as [27]

$$\mathcal{H}_\mu \equiv \langle f |_{out} J_\mu^{em} | 0 \rangle.$$

For reference we include its forms for some final hadronic states in the following. A complete list of \mathcal{H}_μ for all possible two-body final states can be found in Refs. [28, 29].

1. Pseudoscalar-pseudoscalar

For the final states $\pi^+\pi^-$ or K^+K^- ,

$$\mathcal{H}_\mu = \mathcal{F}_P(s)(p_+ - p_-)_\mu,$$

where p_+ and p_- are the four-momentum vectors of π^+ (K^+) and π^- (K^-) respectively, and $\mathcal{F}_P(s)$ is the π or K form factor at the energy scale $s = (p_+ + p_-)^2$.

2. Vector-pseudoscalar

For the VP final states,

$$\mathcal{H}_\mu = \mathcal{F}_{VP}(s)\epsilon_{\mu\alpha\beta\gamma}p_V^\alpha p_P^\beta e^\gamma,$$

with $\epsilon_{\mu\alpha\beta\gamma}$ the completely antisymmetric unit tensor of fourth rank, p_V and p_P are the four-momentum vectors of the vector and pseudoscalar mesons respectively, e is the polarization of the vector meson, $\mathcal{F}_{VP}(s)$ is the form factor at the energy scale $s = (p_V + p_P)^2$.

3. $\pi^+\pi^-\pi^0$ with $\rho\pi$ intermediate states

For the 3-body final states $\pi^+\pi^-\pi^0$,

$$\mathcal{H}_\mu = \mathcal{F}_{3\pi}(s)\epsilon_{\mu\alpha\beta\gamma}p_+^\alpha p_-^\beta p_0^\gamma,$$

with p_+ , p_- and p_0 the four-momentum vectors of π^+ , π^- and π^0 respectively, $\mathcal{F}_{3\pi}(s)$ the form factor at the energy scale $s = (p_+ + p_- + p_0)^2$.

We may also include the three intermediate states $\rho^+\pi^-$, $\rho^-\pi^+$, $\rho^0\pi^0$ and their interference into \mathcal{H}_μ by multiplying a factor

$$\frac{m_\rho^2}{p_{+-}^2 - m_\rho^2 + i\Gamma_\rho(p_{+-}^2)s/m_\rho} + \frac{m_\rho^2}{p_{+0}^2 - m_\rho^2 + i\Gamma_\rho(p_{+0}^2)s/m_\rho} + \frac{m_\rho^2}{p_{-0}^2 - m_\rho^2 + i\Gamma_\rho(p_{-0}^2)s/m_\rho},$$

where m_ρ and $\Gamma_\rho(s)$ are the mass and energy-dependent width of ρ , $p_{+-} = p_+ + p_-$, $p_{+0} = p_+ + p_0$, and $p_{-0} = p_- + p_0$.

APPENDIX B: SOLUTIONS OF $|\mathcal{C}|$ AND ϕ

In this section, we discuss the possible solutions of $|\mathcal{C}|$ and ϕ and so the branching fraction of the resonance decays if the experimental data are available at only two energies, one off the resonance and the other one at the energy of resonance mass. We begin with Eq. (19) and define

$$t^2 = \left| \frac{1}{s(1-x)} + (\mathcal{C}+1) \frac{3\Gamma_{ee}/(\alpha\sqrt{s(1-x)})}{s(1-x) - M^2 + iM\Gamma_t} \right|^2. \quad (\text{B1})$$

Here it is more convenient to consider instead of $|\mathcal{C}|$ and ϕ , the total resonance amplitude by

$$\begin{aligned} \rho &= |\mathcal{C}+1|; \\ \psi &= \arg(\mathcal{C}+1). \end{aligned}$$

Here $\rho = |(a_{3g} + a_\gamma)/a_\gamma|$ is the total resonance amplitude normalized to the electromagnetic amplitude, and $\psi = \arg((a_{3g} + a_\gamma)/a_\gamma)$ is the phase of the total resonance amplitude relative to the electromagnetic amplitude. As discussed in Sec. II, for ψ'' , $|a_\gamma| \ll |a_c|$, so a_γ can be neglected, only the amplitudes of a_{3g} and a_c are important. These two amplitude have significant interference if their magnitude are comparable, i.e.

$$|\mathcal{C}| \sim \frac{\alpha\Gamma_t}{3\Gamma_{ee}} \approx 217.$$

For the discussion on the interference, we only need to consider the circumstance that $|\mathcal{C}| \gg 1$. Then we have

approximately $\rho \approx |C|$ and $\psi \approx \phi$. This means that since $|a_\gamma| \ll |a_c|$, if $|a_{3g}|$ is comparable with $|a_c|$, then $a_{3g} + a_\gamma \approx a_{3g}$, i.e. the total resonance amplitude is approximately equal to the amplitude via strong decay.

For briefness, we introduce the following notations:

$$\begin{aligned} q &= \frac{1}{s(1-x)}, & k &= \frac{3\Gamma_{ee}}{\alpha\sqrt{s(1-x)}}, \\ a &= s(1-x) - M^2, & b &= M\Gamma_t, \end{aligned} \quad (\text{B2})$$

then we have

$$\begin{aligned} t^2 &= \left| q + (|C|e^{i\phi} + 1) \cdot \frac{k}{a+ib} \right|^2 \\ &= \left| q + \rho e^{i\psi} \cdot \frac{k}{a+ib} \right|^2. \end{aligned} \quad (\text{B3})$$

Eq. (B3) can be rewritten as

$$t^2 = q^2 + 2qR \cos(\psi - \lambda) + R^2, \quad (\text{B4})$$

with

$$\begin{aligned} R &= \frac{\rho k}{\sqrt{a^2 + b^2}}; \\ \tan \lambda &= \frac{b}{a}. \end{aligned}$$

To take the radiative correction, we introduce an integral operator defined as

$$\int dG \equiv \int_0^{1-s_m/s} 4\pi s(1-x) \alpha^2 |\mathcal{F}(s(1-x))|^2 \mathcal{P}(s(1-x)), \quad (\text{B5})$$

then the radiatively corrected cross section becomes

$$\sigma_{r.c.}(s) = \int dG t^2 \equiv T^2.$$

Notice

$$qR \cos(\psi - \lambda) \leq qR = \frac{qk}{\sqrt{a^2 + b^2}},$$

and use the relation

$$\left[\int dG qR \right]^2 < \int dG q^2 \cdot \int dG \frac{k^2}{a^2 + b^2},$$

we have

$$\sqrt{A^2 + B^2} \cos(\psi - \Lambda) < QK, \quad (\text{B6})$$

where

$$\begin{aligned} A &= \int dG \frac{aqk}{\sqrt{a^2 + b^2}}, & B &= \int dG \frac{bqk}{\sqrt{a^2 + b^2}}, \\ K^2 &= \int dG \frac{k^2}{a^2 + b^2}, & Q^2 &= \int dG q^2, \end{aligned}$$

and

$$\tan \Lambda = \frac{B}{A}.$$

Introduce a variable ξ and let

$$\cos \xi = \frac{\sqrt{A^2 + B^2}}{QK} \cdot \cos(\psi - \Lambda), \quad (\text{B7})$$

we obtain an expression similar to Eq. (B4):

$$T^2 = Q^2 + 2\rho QK \cos \xi + \rho^2 K^2. \quad (\text{B8})$$

In virtue of Eq. (B7), the angle ξ does not have an apparent physical meaning but has a rather complex relation to the angle ψ .

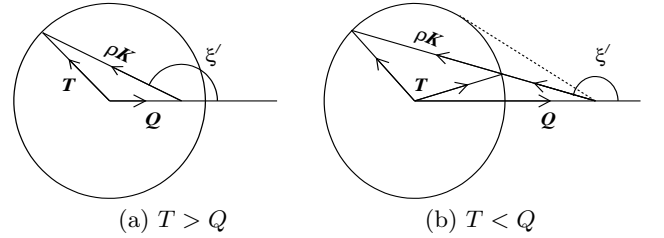


FIG. 5: Possible solutions of ρ and ψ for $T > Q$ (a) and for $T < Q$ (b). Here T , Q , ρK denote the total, continuum and resonance amplitudes, respectively. In the figures $\xi' = \psi' - \Lambda$, where $\psi' = -\psi$ according to the angle definition between two vectors. In (b) the dashed line corresponds to one solution case for special ξ' .

Introduce an angle ζ defined as $\zeta = \pi - \xi$, then Eq. (B8) becomes,

$$T^2 = Q^2 - 2\rho QK \cos \zeta + \rho^2 K^2, \quad (\text{B9})$$

in which the three variables T , Q and ρK form a triangle and obey the law of cosines. If $T > Q$, ζ may take any value between $-180^\circ \sim 180^\circ$, there is one and only one solution for a given value of ζ ; while if $T < Q$, there are two solutions for a value of ζ , but the range of ζ is constrained by $\sin \zeta \leq T/Q$. For $\sin \zeta = Q/T$, the two solutions coincide. In Figs. 5(a) and 5(b) we show schematically the two cases for $T > Q$ and $T < Q$ respectively.

Next we consider the variation of $\epsilon(s_m)$. As discussed in Sec. V, to determine the efficiency by the Monte Carlo simulation, the resonance parameter ρ and ψ are input parameters which are also the quantities to be measured. So the data analysis is an iterative process. Here we are to prove that if the efficiency remains stable for different solutions of ρ and ψ , or with only weak dependence on these two variables, the above discussion is still valid.

In Eq. (B9), T^2 is the total observed cross section, which is obtained by experimentally measured quantities as

$$T^2 = \frac{N}{\mathcal{L} \cdot \epsilon},$$

where the efficiency ϵ is a function of ρ and ψ . Without losing generality, we only write its dependence on ρ explicitly, i.e. $\epsilon = \epsilon(\rho)$. As shown in Sec. V, $\epsilon(\rho)$ remains stable for different solutions of ρ and ψ , and the dependence on these variables is weak, so we take Taylor expansion of ϵ in terms of ρ , and neglect the higher order terms:

$$\begin{aligned}\epsilon(\rho) &= \epsilon(\rho_0) + \left. \frac{d\epsilon(\rho)}{d\rho} \right|_{\rho=\rho_0} (\rho - \rho_0) + \mathcal{O}[(\rho - \rho_0)^2] \\ &\approx \epsilon_0 + \eta\rho = \epsilon_0 \left(1 + \frac{\eta}{\epsilon_0} \rho \right),\end{aligned}$$

where

$$\begin{aligned}\epsilon_0 &= \epsilon(\rho_0) - \left. \frac{d\epsilon(\rho)}{d\rho} \right|_{\rho=\rho_0} \rho_0, \\ \eta &= \left. \frac{d\epsilon(\rho)}{d\rho} \right|_{\rho=\rho_0}.\end{aligned}$$

Here the correction term to ϵ_0 is small, i.e.

$$\frac{\eta\rho}{\epsilon_0} \ll 1. \quad (\text{B10})$$

Therefore we have

$$T^2 = \frac{N}{\mathcal{L} \cdot \epsilon_0 \cdot \left(1 + \frac{\eta\rho}{\epsilon_0} \right)} = \frac{N}{\mathcal{L} \cdot \epsilon_0} \cdot \left(1 - \frac{\eta\rho}{\epsilon_0} \right) = \sigma_t \cdot \left(1 - \frac{\eta\rho}{\epsilon_0} \right), \quad \sigma_t > \frac{(2\delta Q \cos \zeta - 1) + \sqrt{(2\delta Q \cos \zeta - 1)^2 + 4\delta^2 Q^2 \sin^2 \zeta}}{2\delta^2}$$

where we define

$$\sigma_t = \frac{N}{\mathcal{L} \cdot \epsilon_0},$$

with σ_t the total cross section calculated by the efficiency ϵ_0 . Q^2 is the continuum cross section which does not depend on ρ and ψ . Substituting the above expression of T^2 back into Eq. (B9) we have

$$K^2 \rho^2 - \left(2QK \cos \zeta - \sigma_t \frac{\eta}{\epsilon_0} \right) \rho + (Q^2 - \sigma_t) = 0. \quad (\text{B11})$$

We get

$$\rho = \left[(Q \cos \zeta - \delta \sigma_t) \pm \sqrt{(Q \cos \zeta - \delta \sigma_t)^2 + (\sigma_t - Q^2)} \right] / K, \quad (\text{B12})$$

with

$$\delta = \frac{\eta}{2K\epsilon_0}. \quad (\text{B13})$$

Consider the quantity under the radical

$$\begin{aligned}z &= (Q \cos \zeta - \delta \sigma_t)^2 + (\sigma_t - Q^2) \\ &= \delta^2 \sigma_t^2 - (2\delta Q \cos \zeta - 1) \sigma_t - Q^2 \sin^2 \zeta.\end{aligned}$$

In order for Eq. (B12) to have solutions, it requires $z \geq 0$. For $\sigma_t > Q^2$, this is always true. Notice that ρ must be greater than 0 by definition, in this circumstance, ρ has one and only one solution for any given value of ζ , with no constraint on ζ . If $\sigma_t < Q^2$, in order to have $z > 0$, we need the condition

which imposes constraint on ζ . In such case, there are two solutions for each allowed value of ζ . In Eq. (B13), η/ϵ_0 is small, so is δ . In the limit $\delta \rightarrow 0$, we find ρ has two solutions when $Q^2 \sin^2 \zeta < \sigma_t < Q^2$. If $z = 0$, which means

$$\sigma_t = \frac{(2\delta Q \cos \zeta - 1) + \sqrt{(2\delta Q \cos \zeta - 1)^2 + 4\delta^2 Q^2 \sin^2 \zeta}}{2\delta^2},$$

the two solutions of Eq. (B11) becomes one.

-
- [1] J.L. Rosner, Phys. Rev. D **64**, 094002 (2001).
 - [2] P. Wang, X.H. Mo and C.Z. Yuan, Phys. Rev. D **70**, 077505 (2004).
 - [3] P. Wang, C.Z. Yuan and X.H. Mo, Phys. Rev. D **70**, 114014 (2004).
 - [4] CLEO Collaboration, G.S. Adam *et al.*, hep-ex/0509011.
 - [5] BES Collaboration, M. Ablikim *et al.*, Phys. Rev. D **70**, 112007 (2004).
 - [6] BES Collaboration, M. Ablikim *et al.*, Phys. Rev. D **72**, 072007 (2005).
 - [7] P. Wang, C.Z. Yuan and X.H. Mo, Phys. Lett. B **574**, 41 (2004).
 - [8] P. Wang, C.Z. Yuan, X.H. Mo and D.H. Zhang, Phys. Lett. B **593**, 89 (2004).
 - [9] S. Rudaz, Phys. Rev. D **14**, 298 (1976).
 - [10] L. Köpke and N. Wermes, Phys. Rep. **174**, 67 (1989).
 - [11] H.E. Haber and J. Perrier, Phys. Rev. D **32**, 2961 (1985).
 - [12] BES Collaboration, J.Z. Bai *et al.*, Phys. Rev. Lett. **92**, 052001 (2004).
 - [13] CLEO Collaboration, G.S. Adam *et al.*, hep-ex/0510005.
 - [14] F.A. Berends *et al.*, in Proceedings of the Workshop on Z Physics at LEP, v.1, (1989) page 89, edited by G. Altarelli, R. Kleiss and C. Verzegnassi.
 - [15] Particle Data Group, S. Eidelman *et al.*, Phys. Lett. B **592**, 1 (2004).
 - [16] P. Wang, C.Z. Yuan and X.H. Mo, Phys. Rev. D **69**, 057502 (2004).
 - [17] P. Wang, C.Z. Yuan and X.H. Mo, Phys. Lett. B **567**, 73

- (2003)
- [18] Y.S. Tsai, SLAC-PUB-3129 (1983).
 - [19] E.A. Kuraev and V.S. Fadin, *Yad. Fiz.* **41** (1985) 733 [*Sov. J. Nucl. Phys.* **41** (1985) 466]; G. Altarelli and G. Martinelli, *CERN* **86-02** (1986) 47; O. Nicosini and L. Trentadue, *Phys. Lett. B* **196**, 551 (1987); F.A. Berends, G. Burgers and W.L. Neerven, *Nucl. Phys. B* **297**, 429 (1988); *ibid.* **304** (1988) 921.
 - [20] A. Bramon and M. Greco, in *The Second DAΦNE Physics Handbook*, edited by I.Maiani, G. Pancheri and N. Paver, Vol.2, p451, 1995.
 - [21] C.M. Carloni, *Phys. Lett. B* **520**, 16 (2001).
 - [22] A.B. Arbuzov *et al.*, hep-ph/0504233; A.B. Arbuzov *et al.*, *Journal of High Energy Physics* **10**, 006 (1997).
 - [23] H. Czyż and J.H. Kühn, *Eur. Phys. J. C* **18**, 497 (2001).
 - [24] J. Jadach, B.F.L. Ward and Z. Was, *Phys. Rev. D* **63**, 113009 (2001).
 - [25] CLEO Collaboration, N.E. Adam *et al.*, *Phys. Rev. Lett.* **94**, 012005 (2005).
 - [26] BES Collaboration, M. Ablikim *et al.*, *Phys. Lett. B* **614**, 37 (2005); BES Collaboration, M. Ablikim *et al.*, *Phys. Lett. B* **619**, 247 (2005);
 - [27] G. Bonneau and F. Martin, *Nucl. Phys. B* **27**, 381 (1971).
 - [28] Y.S. Tsai, *Phys. Rev. D* **12**, 3533 (1975).
 - [29] Y. Tosa, Nagoya University preprint DPNU-34(1976).